



Supporting Information

Unusual Quartet-Doublet Phosphorescence from the Phosphaethynyl Radical, CP

E. Ganesan, T. Custer, A.-L. Lawzer, J.-C. Guillemin, R. Kotos*

Unusual Quartet-Doublet Phosphorescence from the CP radical

Elavenil Ganesan^a, Thomas Custer^a, Arun-Libertsen Lawzer^{a*}, Jean-Claude Guillemin^b, Robert Kołos^a

a) Institute of Physical Chemistry, Polish Academy of Sciences, Kasprzaka 44/52, 01-224 Warsaw, Poland

b) Univ Rennes, Ecole Nationale Supérieure de Chimie de Rennes, CNRS, ISCR-UMR 6226, F-35000 Rennes, France

Supporting Information

Contents	Page
Experimental details	2
Figure S1. CP luminescence intensity map	3
Figure S2. Decay of the total (undispersed) phosphorescence	3
Figure S3. Decay of $a^4\Sigma^+-A^2\Pi_i$ and $a^4\Sigma^+-X^2\Sigma^+$ emissions	4
Figure S4. The origins of $B^2\Sigma^+-A^2\Pi_i$ and $a^4\Sigma^+-X^2\Sigma^+$ systems	4
Figure S5. Band progression of the $B^2\Sigma^+-X^2\Sigma^+$ systems	5
Figure S6. Simplified schemes of electronic configuration	5
Table S1. The $v'\leftarrow(v''=0)$ progression of the $B^2\Sigma^+-X^2\Sigma^+$ system	6
Table S2. The $(v'=0)\rightarrow v''$ progression in $B^2\Sigma^+-X^2\Sigma^+$ fluorescence	6
Table S3. The $(v'=0)\rightarrow v''$ progression in $B^2\Sigma^+-A^2\Pi_i$ fluorescence	6

Experimental details

As phosphaethyne is highly unstable in its pure form, it was freshly synthesized before each experiment by eliminating HCl from dichloromethylphosphine, $\text{HCl}_2\text{C-PH}_2$, using the strong Lewis base 1,8-diazabicyclo[5.4.0]undec-7-ene (DBU). $\text{HCl}_2\text{C-PH}_2$ was prepared following the published procedure and stored at $-78\text{ }^\circ\text{C}$, either pure or as a solution in diethyleneglycol dibutyl ether (diglyme) [O. Mo, M. Yanez, J.-C. Guillemin, El H. Riague, J.-F. Gal, P.-C. Maria, C. Dubin Poliard, *Chem. Eur. J.* 8 (2002) 4919-4924].

The HCP/Ar mixture was passed through a Granville-Phillips microleak valve and frozen on a sapphire window maintained at ca. 6 K by a DE-202SE cryostat (Advanced Research Systems). A microwave-driven electrodeless xenon discharge lamp (Ophtos Instrument Company, LLC) served as the source of photolytic radiation. The MgF_2 window of the lamp was positioned at a distance of ca. 3 cm from the sample which was then typically irradiated for ~10 to 12 hours. Photolysis progress was monitored by a Shimadzu 2401PC spectrophotometer with its resolution set to 0.5 nm. Dispersed luminescence and luminescence excitation spectra were registered with an FS900CDT spectrofluorimeter (Edinburgh Instruments) equipped with an R955 photomultiplier (Hamamatsu) and a photon-counting system sensitive up to 800 nm. The emission and excitation monochromators have gratings with 1800 grooves/mm. Wavelength calibration errors did not exceed 0.1 nm while the slit width used provided for a resolution of 0.5 nm. The ultimate accuracies of reported band wavenumbers are provided in the Tables. The time decay of the undispersed phosphorescence excited with a 340 nm light-emitting diode was detected by a cooled R955 photomultiplier whose output was recorded with a LeCroy WaveAce 2032 oscilloscope. An alternative method of measuring the emission lifetime involved using a gated CCD camera (Andor iStar DH734) working in tandem with an Omni- λ 300 spectrograph (Gilden, 600 grooves/mm grating). In these measurements, phosphorescence was excited with a 340 nm LED and spectra were measured with adjustable delays (step of 10 ms, gatewidth 10 ms) after switching the excitation light off. The wavelength-resolved approach allowed for measurement of the decays of individual phosphorescence features.

Preparation of phosphaethyne (HCP). Dichloromethylphosphine (0.2 g, $-50\text{ }^\circ\text{C}$) was slowly added via a flexible needle, under inert gas atmosphere, to a solution of DBU (0.8 g) in diglyme (40 mL) kept at $-65\text{ }^\circ\text{C}$. The reaction mixture was then cooled to $-110\text{ }^\circ\text{C}$, pumped out, and slowly warmed. As the mixture melted, the released HCP gas was passed through a U-shaped trap ($-110\text{ }^\circ\text{C}$) into an evacuated chamber, where it was mixed with argon using standard manometric techniques.

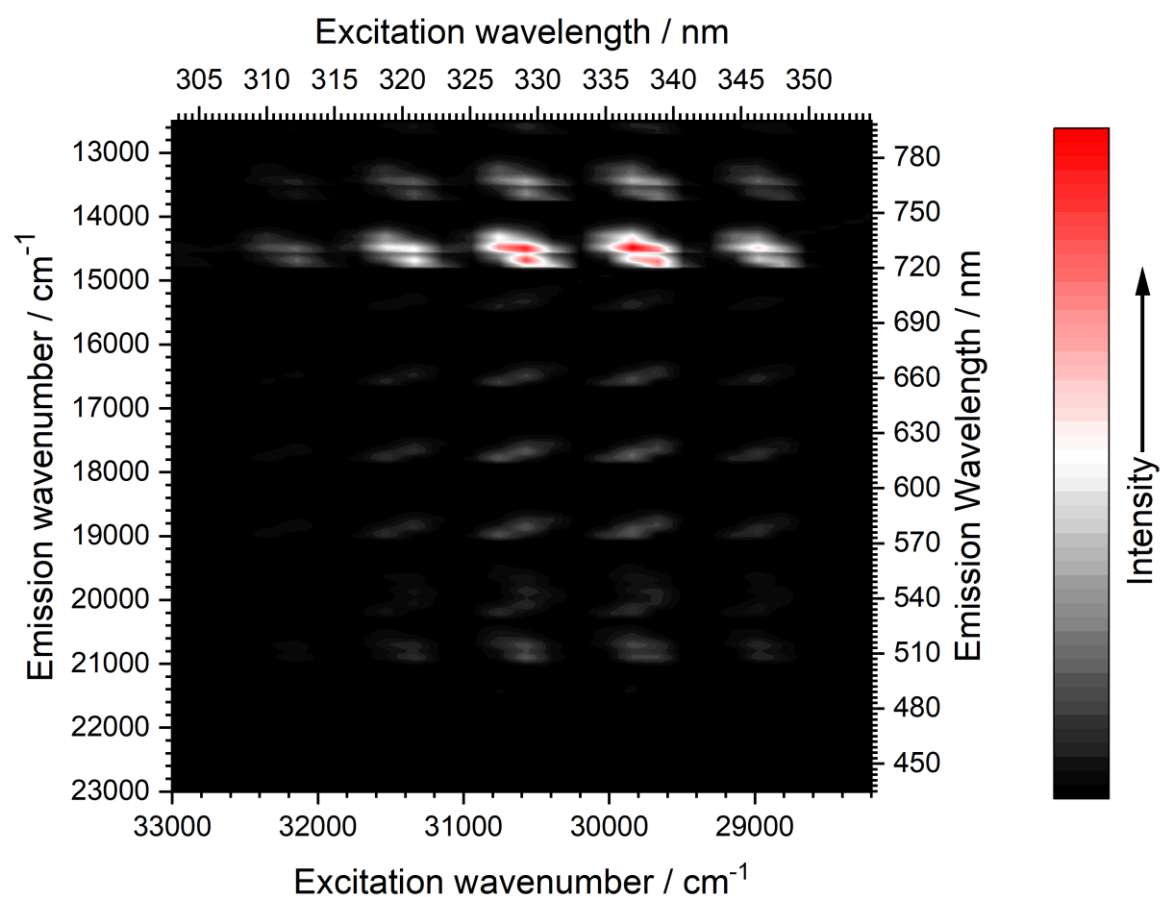


Figure S1. Luminescence of CP in solid Ar, mapped as a function of excitation and emission wavelength/wavenumber.

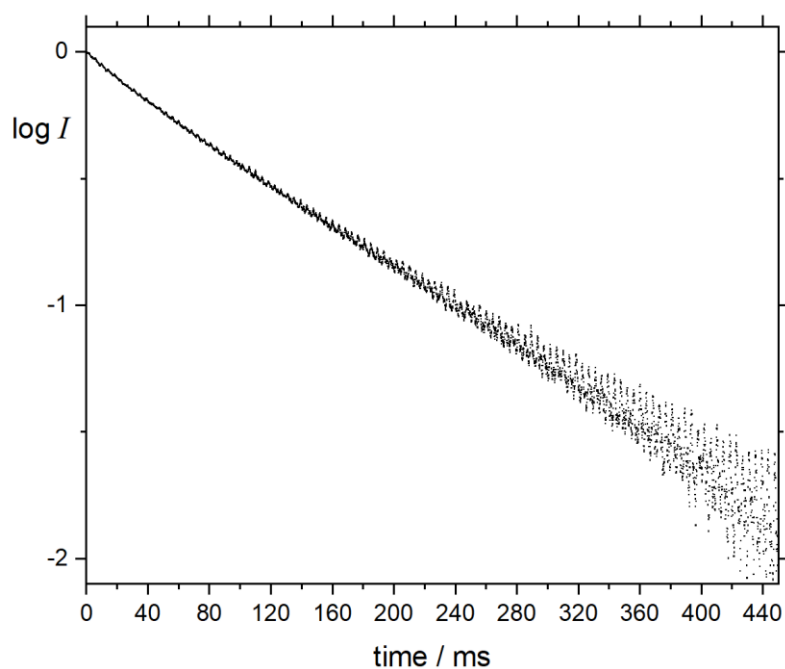


Figure S2. Decay of the logarithm of the total phosphorescence intensity, as observed for Ar matrix-isolated CP after switching off the 340 nm LED excitation source.

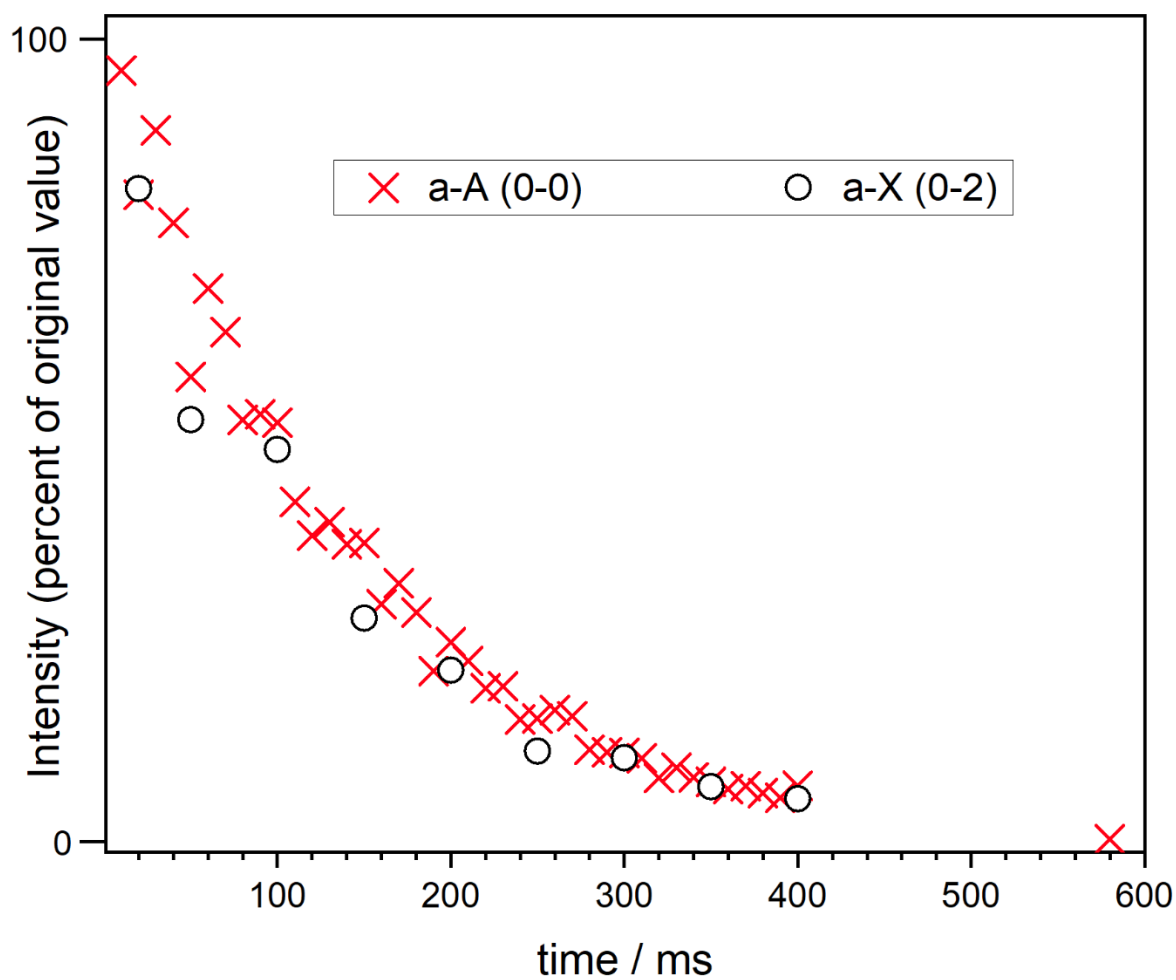


Figure S3. Decay of intensity for separately measured $a^4\Sigma^+-A^2\Pi_1$ ($v'=0$) \leftarrow ($v''=0$) and $a^4\Sigma^+-X^2\Sigma^+$ ($v'=0$) \leftarrow ($v''=2$) phosphorescence bands.

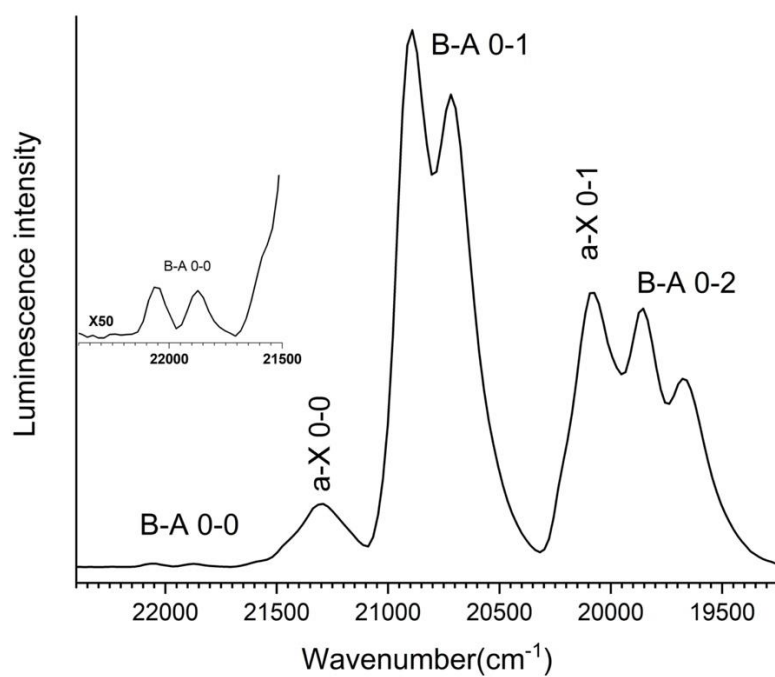


Figure S4. The origins of the $B^2\Sigma^+-A^2\Pi_i$ and $a^4\Sigma^+-X^2\Sigma^+$ emission systems of CP in solid Ar following $B^2\Sigma^+ \leftarrow X^2\Sigma^+$ ($v'=1 \leftarrow (v''=0)$) excitation ($29\,700\text{ cm}^{-1}$).

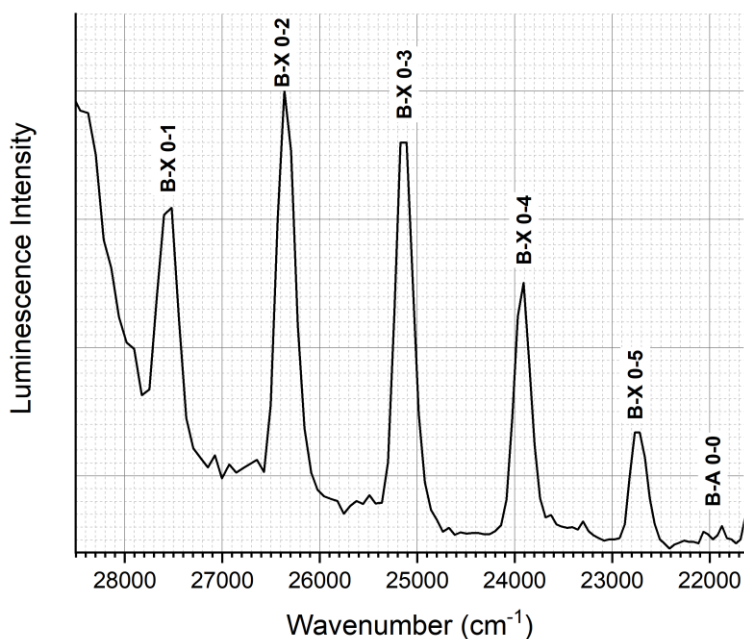


Figure S5. Band progression in $B^2\Sigma^+-X^2\Sigma^+$ fluorescence of CP in solid Ar following $B^2\Sigma^+ \leftarrow X^2\Sigma^+$ ($v'=3 \leftarrow (v''=0)$) excitation ($31\,250\text{ cm}^{-1}$). See Tab. S2.

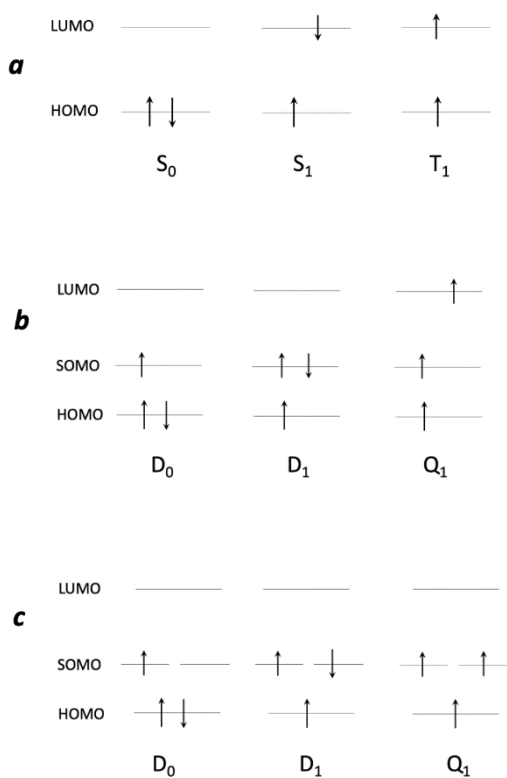


Figure S6. Simplified schemes of the electronic orbital configuration for: (a) the lowest singlet and triplet states of a closed-shell molecule; (b) the lowest doublet and quartet states of a free radical; (c) a free radical with a degenerate ground state (example: NO radical). HOMO, SOMO, and LUMO stand for the highest occupied, singly occupied, and lowest unoccupied molecular orbitals, respectively. Schemes explain why the lowest excited electronic state is T_1 in

case (a), D₁ in (b), and Q₁ in (c). Free radicals usually adhere to (b). Hund's rule is responsible for the order of states in (a) and (c).

Table S1. The $v' \leftarrow (v''=0)$ progression of the $B^2\Sigma^+-X^2\Sigma^+$ system, as observed in absorption and phosphorescence excitation spectra of CP in solid Ar. All values in cm^{-1} .

v'	Ar matrix ^a		Gas phase ^b
	$X^2\Sigma^+-B^2\Sigma^+$ absorption ^c	Phosphorescence excitation ^c	$B^2\Sigma^+-X^2\Sigma^+$ fluorescence
0	28 900	28 930	28900
1	29 760	29 795	29722
2	30 580	30 660	30538
3	31 350	31 430	31337
4	32 150	32 240	32126
5	33 000	32 990	32900
6	33 790	33 770	33671

^a) This work, sample annealed at 25 K.

^b) Band head positions reported by V.H. Bärwald, G. Herzberg, L. Herzberg, *Ann. Phys.*, **1934**, 20, 569–593.

^c) Measurement accuracy changes from $\pm 20 \text{ cm}^{-1}$ at the top to $\pm 30 \text{ cm}^{-1}$ at the bottom.

Table S2. The $(v'=0) \rightarrow v''$ progression in $B^2\Sigma^+-X^2\Sigma^+$ fluorescence of CP in solid Ar upon $B^2\Sigma^+ \leftarrow X^2\Sigma^+ (v'=3) \leftarrow (v''=0)$ excitation ($31\,250 \text{ cm}^{-1}$) and compared with gas-phase data. All values in cm^{-1} . See Fig. S4.

v''	Ar matrix ^a	Gas phase ^b
0	28 900 ^c	28 900
1	27 520	27 675
2	26 360	26 462
3	25 140	25 264
4	23 910	24 079
5	22 750	

^a) Measurement accuracy changes from $\pm 20 \text{ cm}^{-1}$ at the top to $\pm 15 \text{ cm}^{-1}$ at the bottom.

^b) Band head positions reported by V.H. Bärwald, G. Herzberg, L. Herzberg, *Ann. Phys.*, **1934**, 20, 569–593.

^c) As indicated by the absorption spectrum (*cf.* Table S1).

Table S3. The $(v'=0) \rightarrow v''$ progression in $B^2\Sigma^+-A^2\Pi_i$ fluorescence of CP in solid Ar upon $B^2\Sigma^+ \leftarrow X^2\Sigma^+ (v'=1) \leftarrow (v''=0)$ excitation ($29\,700 \text{ cm}^{-1}$). All values in cm^{-1} . Upper and lower values correspond to $\Omega=1/2$ and $\Omega=3/2$ sublevels of the $A^2\Pi_i$ state, respectively.

v''	Wavenumber ^a
0	22 040
	21 870
1	20 890
	20 720
2	19 850

19 660

a) Measurement accuracy $\pm 10\text{ cm}^{-1}$.